Propellant Interaction with the Payload Control System of Dual-Spin Spacecraft

Loren I. Slafer* and A. Dorian Challoner†
Hughes Aircraft Company, El Segundo, California

Significant interaction between the payload control system and the liquid propellant on dual-spin spacecraft is shown to exist for a new class of vehicles with large liquid mass fractions. Experience during the transfer orbit operations of the first two LEASAT synchronous orbit communications satellites has demonstrated that lateral sloshing modes within the propellant can become unstable when coupled to the payload control system. Scaled-model single-axis transfer function testing is shown to define critical propellant modal parameters accurately. Analytical modeling techniques using this propellant modal test data are presented that can be used to predict both the strength and basic stability of the interaction. Design guidelines are presented for use in selecting system parameters to ensure stability. On-orbit verification of the interaction hypotheses, validating the test data and analytical modeling, is demonstrated with results of experiments conducted on the third LEASAT spacecraft.

Nomenclature

a_T	= radius of propellant tank
d_T	= radial distance from vehicle spin axis to tank center
DCS	= despin control system
FF	= propellant tank fluid fraction fill
I_i	= ith liquid mode coupling inertia about spin axis
I_p	= payload MOI about spin axis
I_R	= dry rotor MOI about spin axis
I_s	= rotor MOI about spin axis (including liquid)
I_0	= total liquid MOI about spin axis
J	= I_p/I_s
K_∞	= rotor transfer function gain (T_s/ω_3)
ℓ_1, m_1	= first-mode equivalent pendulum length and mass, respectively
m_L	= total liquid mass
m_∞	= residual liquid mass ($m_L - m_1$)
MOI	= moment of inertia
r	= mass property coupling parameter, $= J\rho/(1+J-\rho)$
s	= Laplace variable
T_3	= bearing axis torque, $= T_{\mathrm{BA}}$
θ_R	= payload-to-rotor relative phase angle
ξ_{cl}	= propellant damping ratio due to closing control loop
ξ_{net}	= $\xi_{\mathrm{cl}} + \xi_p$
ξ_p	= passive fluid damping ratio
ρ	= propellant mass coupling factor ($= nI_1/I_s$)
ω_1	= natural frequency of first (azimuth) mode

I. Introduction

THE LEASAT synchronous orbit communications satellite (shown in Fig. 1) represents the first in a new class of dual-spin spacecraft being developed that rely on liquid propulsion for a significant portion of their required orbital adjustment maneuvers. Others in this class include the INTELSAT VI and Hughes' HS-393 series communications satellites and the Galileo spacecraft. These dual-spin configurations comprise 1) a spinning portion (the rotor) providing basic gyroscopic attitude stabilization for the spacecraft and containing the propulsion subsystem and 2) a mechanically despun payload. Continuous active control of the payload is provided to maintain either a constant inertial spin rate or fixed inertial pointing direction. A unique feature of this class of spacecraft is the large liquid mass fraction of the rotor existing over a major portion of the mission. At launch, LEASAT contains 4100 lb of liquid bipropellant in four 96% full, 36 in. diam propellant tanks (two fuel and two oxidizer). For LEASAT, the tank centers are located radially outboard, 5 ft from the spacecraft spin axis. The dry LEASAT rotor weight is only 1800 lb. The bipropellant propulsion system for INTELSAT VI includes initially 6000 lb of liquid propellant contained in eight 33 in. diam tanks, located 4 ft from the spin axis. The dry rotor weight in INTELSAT VI is 1650 lb.

A second characteristic of this new class of spacecraft is the configuration of the despin control system (DCS) used for rate and position control of the mechanically despun payload. The systems make use of a shaft angle encoder contained in the despin bearing assembly to provide relative, payload-to-rotor phase and rate information to the control system. Control of the payload is achieved through use of electric torque motors also contained in the bearing assembly. Thus, a significant characteristic of these spacecraft is the direct inclusion of the rotor dynamics within the control system.

During transfer orbit operations of the first LEASAT mission (in September 1984), a control system instability developed during the preapogee injection phase, immediately following activation of the despin control system. Details of this anomaly are presented in Sec. II. Once on orbit, no anomalies were observed and the spacecraft control system performed normally. This instability was observed again during transfer orbit operations of the second LEASAT launched two months later.

As a result of the initial LEASAT experience, a study was undertaken to explain the source of the instability. Previous analyses and testing had shown the payload and rotor structural modes to be only weakly coupled to the control system and the interaction to be stable in the presence of the measured 0.7% structural damping. The investigations pointed to propellant oscillations as the most probable cause of the instability. Propellant dynamics had not been originally considered in the design because the initial mission plan had maintained the payload and rotor in a locked configuration until achieving geosynchronous orbit. The mission plan described in Sec. II was modified prior to launch to avoid other dynamic problems.

Received June 1, 1987; revision received Sept. 21, 1987.

*Laboratory Scientist, Guidance and Control Systems Laboratory, Space and Communications Group. Member AIAA.

†Senior Project Engineer, Guidance and Control Systems Laboratory, Space and Communications Group.

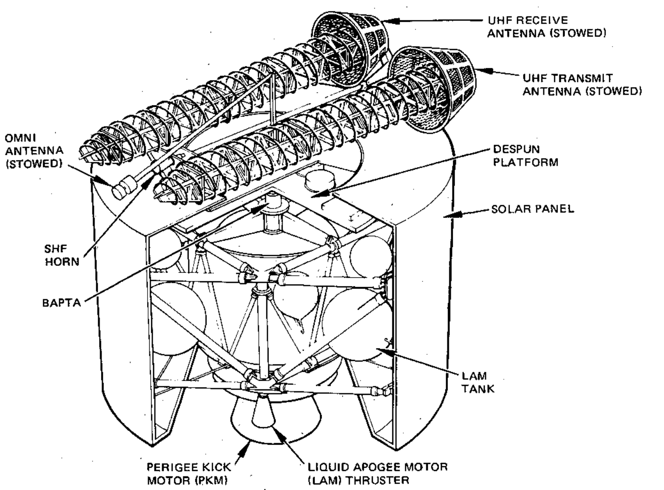

Fig. 1 LEASAT synchronous orbit communications satellite.

The LEASAT investigations demonstrated that, just as flexible elements on the payload can interact stably or unstably with the payload control system, for a control system utilizing relative, rotor-to-payload phase and rate data, lateral sloshing of the propellant can become strongly coupled to the control system—a problem similar to the one identified during the 1960's in the design of attitude control systems for launch vehicles.[2] Coupling to the despin control system develops when control torques about the bearing axis excite what will be shown in Sec. III to be lateral sloshing modes within the propellant. The reaction of the rotor to these azimuthal propellant oscillations is a sinusoidal modulation of the rotor spin rate at slosh mode frequencies. Variations in rotor spin rate are sensed directly by the control system through the shaft encoder and, for linear system operation, feedback control torques will then be generated at the sensed oscillation frequency. Depending upon the characteristics of the transmission of the propellant slosh frequency through the control loop, this interaction can become either stabilizing or destabilizing.

Because of two primary factors arising from the large tank size, propellant interactions can become significantly more severe than the generally higher-frequency mechanical structural mode interactions. These factors are:

1) Extremely low passive damping within the fluid. On-orbit measurements on the LEASAT spacecraft show propellant damping (with unbaffeled tanks) to be less than 0.05% (an order of magnitude weaker than structural damping).

2) The extremely high dynamic inertia ratio of the propellant mode (i.e., the ratio of the effective moment of inertia of the propellant mode to the total rotor moment of inertia) resulting from large liquid mass fractions.

The propellant interaction for LEASAT was demonstrated in simulation studies that modeled the propellant as two-degree-of-freedom pendulums attached to a rigid, spinning rotor, with one pendulum for each propellant tank. The initial pendulum model (a "rigid slug" model) assumed the fluid to be a distributed mass, pivoting about the center of the tank with the pendulum mass located at the fluid mass center. These studies demonstrated the interaction phenomenon, but failed to predict the instability (characterized by the oscillation frequency and closed-loop propellant damping ratio) observed during both LEASAT missions.

A more sophisticated "modal" model was then developed, utilizing the lateral slosh modes within the propellant. This model, in conjunction with scale-model testing, accurately predicted the LEASAT behavior. This analysis was then confirmed through experiments conducted during the third LEASAT mission.

This paper presents the results of the investigations into the propellant interaction phenomenon carried out to explain the LEASAT anomaly, as well as to develop analytical techniques and design guidelines for the development of control systems on future spacecraft of this class. Section II presents details of the anomaly observed during the first two LEASAT missions. Analytical modeling of lateral slosh modes and scaled-model testing to determine critical modal parameters are described in Sec. III. Section IV presents a closed-loop interaction analysis, describing a closed-form solution to the propellant interaction problem, providing both an analytical technique to characterize the interaction and design criteria to ensure loop stability. The results of a series of experiments conducted on the third LEASAT mission to verify the results of the analysis and testing are presented in Sec. V.

II. LEASAT Transfer Orbit Anomaly

In the mission sequence for LEASAT[1] the spacecraft is ejected from the shuttle with the payload and rotor mechanically locked together. A solid rocket motor places the spacecraft into a low altitude (8300 n.mi.) elliptical subtransfer orbit. Three ground commanded firings of the two 100 lbf bipropellant system thrusters at perigee are carried out to raise apogee to the 19,300 n.mi. altitude required for synchronous orbit injection. These maneuvers use $\sim$1300 lb of the initial 4100 lb propellant load. The mission plan then calls for transition to a dual-spin mode of operation by releasing the locking mechanisms that hold the two bodies together and despinning the payload through the use of the electric torque motors. The amount of bipropellant remaining at this point in the mission is $\sim$62%. All bipropellant thruster firings at apogee are then carried out in a relative rate control mode.

Following initial despin of the payload during the launch of the first LEASAT spacecraft (and as observed during all subsequent missions), a control system instability developed requiring use of a backup ground control mode during transfer orbit operations. Spacecraft telemetry showing the control system response during this first anomaly is given in Fig. 2. The figure presents time histories of the control system telemetry response during the initial despin maneuver. Once the launch locks are released and the payload is free to rotate, torque motors are activated to initiate despin. Because of a large payload unbalance, the spacecraft will develop 1–2 deg of nutation during the despin maneuver as the payload passes through the nutation resonance condition. Once the payload is despun, with the DCS holding the payload at a controlled low ($\sim$1 rpm) inertial spin rate, the combined effects of passive fluid tube nutation dampers and the DCS coupling through the platform unbalance[3] act to remove the induced nutation. However, as can be seen in Fig. 2, once the nutation amplitude had been reduced to a level that does not result in saturation of the despin motors, both the servo error signal and motor torque amplitude begin to grow exponentially, driving the motor back into saturation. High-frequency oscillatory growth can also be seen in the rotor spin period and measured solar aspect angles (traces 1 and 2) derived from rotor-mounted slit-type sun sensors.[1] Once the oscillation had grown sufficiently large to saturate the motor, a backup ground control mode was activated by command.

This mode uses the inherent rate feedback of the constant-voltage torque motor drive circuitry to create an extremely low bandwidth passive rate control loop (with a time constant of $\sim$40 min). With the active control loop broken, the rotor oscillations are seen to damp out exponentially with a time constant of $\sim$500 s.

Several other transitions from backup to primary control without initial nutation were made with identical results (i.e., unstable exponential growth within the control system). This maneuver was repeated after each 30 min apogee firing of the bipropellant system, with instability resulting at each condition until following the final firing. After the last bipropellant system firing, the amount of bipropellant had been reduced to less than 150 lb ($<$3% fill fraction). With the propellant nearly depleted, the control system operated normally and no additional instabilities developed.

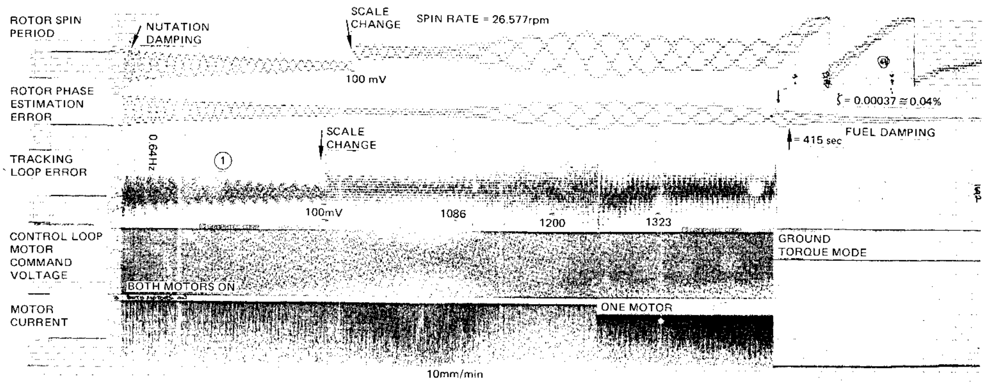

Fig. 2 LEASAT spacecraft telemetry during first observed instability.

III. Spinning Propellant Modal Identification

The spinning liquid-propellant modes that can significantly interact with a spacecraft despin control system are readily identified using a single scale model propellant tank mounted on a spin table. Measurement and analysis of an appropriate mechanical transfer function that is sensitive to the liquid reaction torques can provide accurate estimates of the liquid mode frequencies, coupling inertias, and damping ratios. These modal parameters can be readily scaled and employed with the specific spacecraft dry rotor inertia to yeild the required rotor torque transfer function for despin control system analysis. This approach is not dependent on modeling of the internal liquid behavior, which is quite appropriate in view of the absence to date of any reliable published theory on the partially filled off-axis tank, the most common spinning spacecraft configuration.

Modal Analysis

Our objective in this section is to model the spacecraft rotor despin control torque transfer function $[\omega_3/T_3]$, relating the three-axis (spin axis) rate variations ω_3 to the applied three-axis torques T_3 and particularly any deviations from the previously assumed rigid response: $[\omega_3/T_3]_{\text{rigid}} = 1/sI_s$.

In principal, this could be accomplished by ground test of a scaled four-tank rotor model spun at sufficiently high speed ω_s to closely approximate the 0 g free surface condition of flight. By preserving the flight ratio of tank diameter to radial offset and of liquid-to-dry spin inertia, the ground-measured transfer function of the rotor rate to the torque would be that of the flight vehicle within the test inertia and spin frequency scale factors. Accurate matching of the amplitude at slosh resonances, i.e., modal damping, could also be obtained if the flight Reynolds number $Re = \omega_s d^2/\nu$ were maintained in the test, where d is the tank diameter and ν the kinematic viscosity of the liquid.

In practice, it is convenient to test only a single small-scale tank and not have to match the flight liquid/rigid inertia ratio. Also, with small tanks, it is found that the spin speed (at which 0 g convergence is achieved relative to modal frequency and coupling inertia) is considerably lower than that required for matching flight Reynolds number or modal damping. The latter parameter is often not as critical for initial control system analysis, thus allowing a lower test spin speed and reduced centrifugal design loads. We can operate in this more expedient manner with a single tank by applying the methods of modal analysis and test of lightly damped structures.

To do this, we first write the measured transfer function as

$$\left[\frac{T_3}{\omega_3}\right] = K_\infty s \,\Pi \left(\frac{s^2 + 2\zeta_i^* \omega_i^* s + \omega_i^{*2}}{s^2 + 2\zeta_i \omega_i s + \omega_i^2}\right) \tag{1}$$

where the parameters of $[T_3/\omega_3]$ are selected to provide the best fit with the measurement data. A variety of parameter estimation techniques are available from simple single-degree-of-freedom manual methods to automated multi-degree-of-freedom algorithms requiring little manual support.[4] A liquid inertia $I_L(s)$ can then be defined and the response of the spin table dry inertia I_R can be readily removed, as

$$I_L(s) = \left(\frac{1}{s}\right)\left[\frac{T_3}{\omega_3}\right]^* - I_R = I_0 - \Sigma \frac{I_i s^2}{(s^2 + \omega_i^2)} \tag{2}$$

where $[T_3/\omega_3]^*$ is simply Eq. (1) without damping and

$$I_0 = I_s - I_R$$
$$I_s = K_\infty \,\Pi\, (\omega_i^*/\omega_i)^2$$
$$I_i = K_\infty \,\Pi \left[\frac{(\omega_j^*/\omega_i)^2 - 1}{\pi[(\omega_j/\omega_i)^2 - 1]}\right], \qquad j \neq i$$

The elimination of damping (which is typically $<1\%$) leads to negligible error in determination of the modal coupling inertias I_i. With these modal parameters identified, we may now account for the actual number of tanks n and rigid inertia of the flight rotor and generate the required despin torque transfer function $[\omega_3/T_3]$ by reversing the role of Eq. (2). For example, if we assume a single dominant liquid mode as in the original LEASAT investigation, we have

$$\left[\frac{\omega_3}{T_3}\right] = \frac{(s^2 + \omega_1^2)}{sI_s[(1-\rho)s^2 + \omega_1^{*2}]}, \qquad \rho = nI_1/I_s \tag{3}$$

where I_1 is the modal inertia for the flight propellant up-scaled from the test value by the ratio of $m_L d_T^2$, using the average mass of the flight liquid (oxidizer and fuel), for the value of m_L in the flight case and I_s is the estimated flight rotor total rigid-body spin inertia.

The pole/zero ratio in Eq. (3), $1/\sqrt{1-\rho}$, is significantly different from 1 for $\rho \to 1$, i.e., for relatively large liquid-to-rigid inertia ratios. For a spherical tank, the most sensitive modal test is to measure the tank lateral reation force rather than the table torque since the effective rigid inertia is $I_R = m_T d_{T2}$, where m_T is the relatively lightweight tank mass (typically 10% of the full liquid mass). Because of the inviscid liquid assumption and spherical tank shape, there is no significant liquid reaction torque to measure about the tank center.

To facilitate comparison with nonspinning 1 g lateral slosh data[2] and other data, it is convenient to relate the measured azimuth-coupled modal parameters to those of a simple spinning pendulum model illustrated in Fig. 3. It comprises a pendulum point mass m_1 suspended from a pivot P assumed to be located at the tank center, which is at distance d_T from the spin axis. The remainder of the fluid mass m_∞ is assumed to be rigid and located at point P (which is consistent for an inviscid fluid) and the total fluid mass m_L is centered at distance ℓ_{cm} from P.

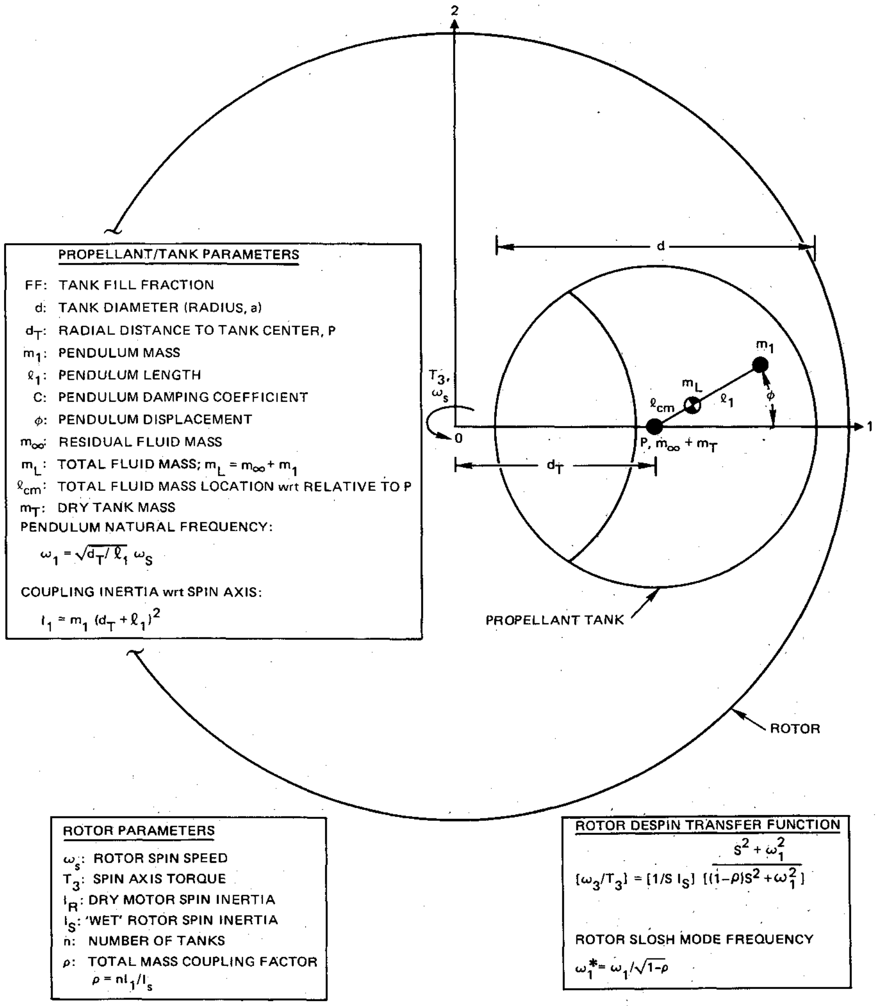

Fig. 3 Simple azimuth slosh pendulum model.

(Note that for this model $\ell_{cm} = m_1\ell_1/m_L$.) Other useful pendulum and rotor parameters are also defined in the figure.

The linearized equations for the lateral tank reaction force and spin axis torques about P can be derived as, respectively.

$$m_T d_T \dot\omega_3 + \{m_\infty d_T \dot\omega_3 + m_1(d_T + \ell_1)\dot\omega_3 + m_1\ell_1\ddot\phi - m_1\omega_s^2\ell_1\phi\} = 0 \tag{4a}$$

$$m_1(d_T + \ell_1)\ell_1\dot\omega_3 + m_1\ell_1^2\ddot\phi + m_1 d_T\ell_1\omega_s^2\phi = 0 \tag{4b}$$

which leads through routine transfer function analysis to

$$\left[\frac{F_2}{\omega_3}\right] = s\left[\left(\frac{I_s}{d_T}\right) - \frac{(I_1/d_T)s^2}{(s^2+\omega_1^2)}\right] \tag{5}$$

where

$$\omega_1^2 = \left(\frac{d_T}{\ell_1}\right)\omega_s^2 \text{ normalized mode frequency } \omega_1 = \sqrt{\frac{d_T}{\ell_1}}$$

$$I_1 = m_1(d_T + \ell_1)^2$$

$$I_s = m_T d_T^2 + I_0$$

$$I_0 = m_\infty d_T^2 + m_1(d_T + \ell_1)^2 = m_L(d_T + \ell_{cm})^2$$

Clearly, ℓ_1 and m_1 may be selected to match the measured transfer function data for ω_1 and I_1; however, there is no guarantee of a match for I_0, the total liquid moment of inertia, since there is no further freedom in the model ($\ell_{cm} = m_1\ell_1/m_L$). If the internal liquid behavior is irrotational, as it would be in a uniform gravitational field without spin, then the pendulum analogy is known to be correct so I_0 is in fact matched.[2]

Finally, with good separation between pole and zero frequencies and low damping ζ_1, is is possible to obtain $[m_1/m_L]$ directly from the measured transfer function as

$$\left[\frac{m_1}{m_L}\right] = \left[\frac{\hat\omega_1^2}{(1+\hat\omega_1^2)^2}\right]\left(\frac{\Delta}{m_L d_T \omega_s^2}\right)\left[\frac{F_2}{\omega_3}\right]_{\max} \tag{6a}$$

where $\Delta = 2\zeta_1\omega_1$ is the 3 dB width of the measured transfer function. An alternate derivation of m_1 depending only on the pole/zero frequency ratio and estimated torque transfer function gain K_∞ follows from a comparison of Eqs. (3) and (5) (multiplied by d_T and inverted) as

$$\left[\frac{m_1}{m_L}\right] = \left[\frac{\hat\omega_1^2}{(1+\hat\omega_1^2)}\right]^2\left[\frac{K_\infty}{m_L d_T^2}\right]\left[\left(\frac{\omega_1^*}{\omega_1}\right)^2 - 1\right] \tag{6b}$$

Further, if a gain estimate is not available it can be calculated from Eq. (2) as

$$K_\infty = [m_T d_T^2 + I_0](\omega_1/\omega_1^*)^2$$

using the approximation $I_0 = m_L(d_T + \ell_{cm})^2$, which is exact for a true pendulum type mode. For relatively large radial offset, the planar surface spherical segment *cm* location could be employed for ℓ_{cm}. Note that, with $d_T/\ell_1 = \hat\omega_1 \to \infty$, the uniform g pendulum result is obtained, i.e., $\omega_1 \to \sqrt{g/\ell_1}$ and m_1/m_L follows from Eq. (6).

Modal Test Method

The test setup to measure $[F_2/\omega_3]$ is depicted in Fig. 4. The key element on the spin table is the 4 in. plastic sphere partially filled with water and mounted via load cell supports at the desired radial offset. On the nonspinning side the essential equipment comprises a spectrum analyzer and X-Y recorder.

Excitation level was adjusted to produce an approximate small rate table motion of ± 0.1 in. rms to ensure linear behavior; the analyzer coherence display was also monitored periodically to ensure excessive excitation was not employed. Instrument frequency resolution was 0.04 Hz and amplitude accuracy was ± 1 dB. A Hanning window function was selected with typically 16 averages being obtained before the amplitude transfer function was output to the X-Y recorder.

Test Results

First, the transfer function $[F_2/\omega_3]$ of tank lateral reaction force to table rate at zero spin speed and FF = 65% in Fig. 5a serves to validate the test method. In a uniform 1 g field, the frequency of a pendulum of length a, the tank radius is $f_0 = \sqrt{g/a}/2\pi = 2.21$ Hz, the tank characteristic frequency. Following the practice in the liquid slosh literature, the observed resonance frequencies are normalized to f_0 and are noted as $\eta_1 = 1.34$ and $\eta_2 = 2.42$ on Fig. 5a. These values compare well with those established for the spherical tank modes (e.g., $\eta_1 = 1.34$ and $\eta_2 = 2.33$, estimated from Fig. 6-20 of Ref. 2). For the first and dominant mode, the equivalent simple pendulum model mass m_1 can be obtained from Fig. 5a in one of two ways as discussed above. One uses an estimate of mode damping from the 3 dB width, while the second method uses an estimate of the pole/zero ratio (zero estimated as 3.70 Hz from the original curve). Both give similar values in this case with the latter method [Eq. (6b)] yielding $m_1/m_L = 0.44$ against the published value of $m_1/m_L = 0.46$ (Ref. 2, Fig. 6-20). [The tank mass, $m_T = 0.13\, m_L$ and liquid center of mass $\ell_{cm} = 0.265a$ for use in Eq. (6b).]

Figures 5b and 5c next illustrate the same transfer function (with unscaled logarithmic amplitude) at a sufficiently high spin speed $f_s = 3.056$ Hz to identify the first two modes, f_1 and f_3, that are significantly coupled to spin rate variations in the pure spin condition; a small degree of coriolis coupling with the first elevation mode f_2 is still apparent at this Froude number ($Fr = d_T\omega_s^2/g = 6.47$), but has negligible effect on f_1 and f_3. In this case, the reported mode frequencies ω_i are more conveniently normalized to spin speed and the first azimuth slosh mode frequency is thus identified as $\omega_1 = 2.15$. It has been far the largest azimuth coupling, as evidenced by the wide separation between pole and zero frequencies, at 6.56 and 7.82 Hz, respectively, which determine the mode mass [Eq. 6b]. Averaging these data with that of a second test run ($f_p/f_z = 6.60/7.80$), the mode frequency and mass predictions are summarized as $\omega_1/\omega_s = 2.153$ and $m_1/m_L = 0.26$. Data were also taken at lower Froude numbers to confirm that a 0 g limit had been obtained.

Figure 6 summarizes the trends for all of the test data taken with this original test setup at the LEASAT radial offset location ($d/d_T = 0.59$), along with the predictions of the two ad hoc pendulum models used shortly after the LEASAT anomaly to formulate the propellant slosh interaction hypothesis. The first

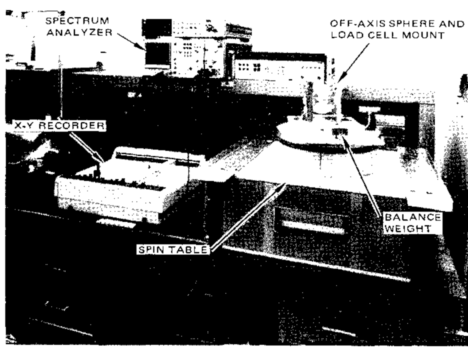

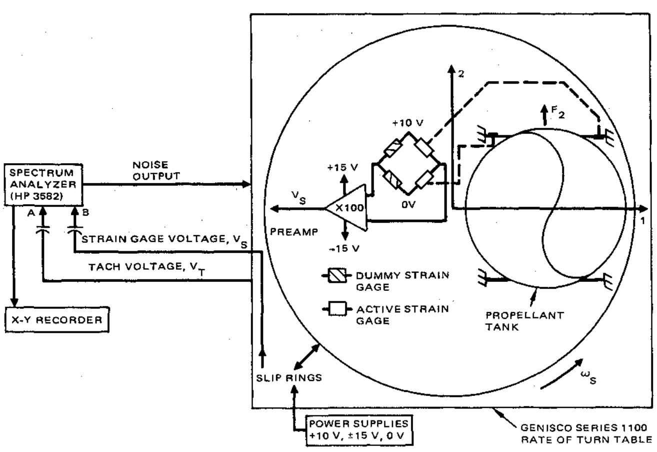

Fig. 4 Spinning propellant modal test setup (single-axis).

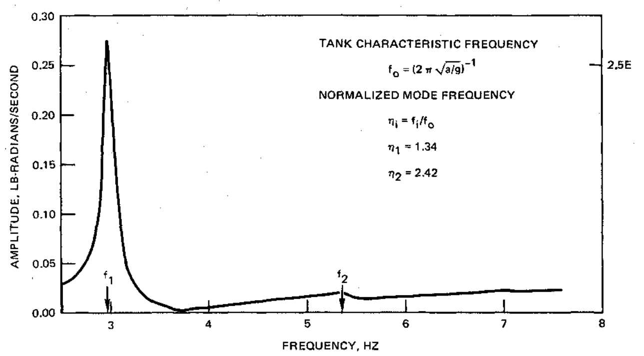

a) Nonspinning (1 g), linear amplitude

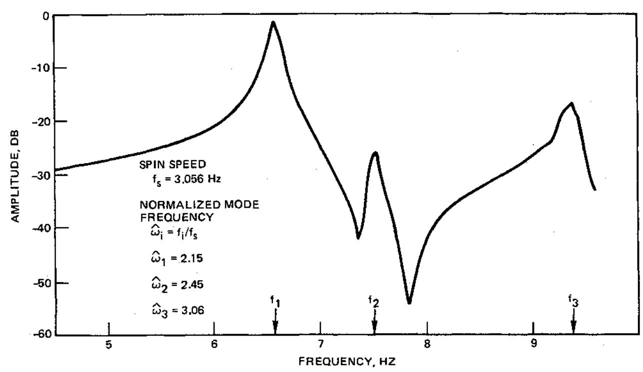

b) Spinning (1100 deg/s), logarithmic amplitude

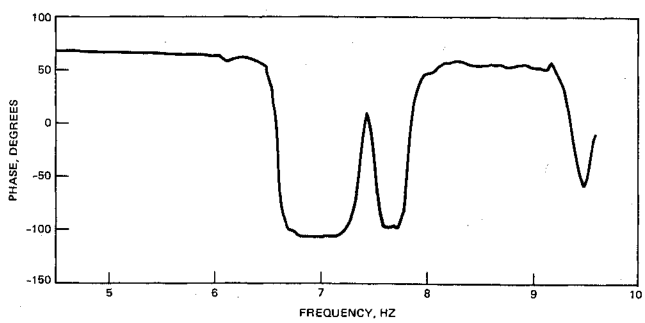

c) Phase

Fig. 5 Measured azimuth transfer function $[F_2/\omega_3]$ at 65% FF $d/d_T = 0.59$.

model considered, the rigid spherical segment pendulum, has had prior application in various simulations and static stability analyses at Hughes. As we can see in the figure, its frequency prediction is sharply lower than test data above 50% FF and, in fact, rapidly tends to zero while the test data rapidly increases and, as we shall see in Sec. IV, fails to predict the observed flight instability. The second ad hoc model, based on established nonspinning uniformity gravity slosh data, was advanced to maintain support for the slosh interaction hypothesis despite the failure of the rigid slug model simulations. It plainly assumes that the surface curvature and Coriolis forces present in the spinning case can be neglected and that the uniform gravity (nonspinning 1 g) slosh pendulum mass and length can be used directly. This model characteristically shows significantly higher mode frequencies and mass than spinning test data at all fill fractions; however, it appears more realistic in that it correctly predicts the mode frequency and mass trends vs fill fraction in the test data.

The LEASAT rotor slosh mode frequency predicted ω_1^* with these three propellant slosh models are summarized in Table 1. The significant conclusion is that the rotor mode frequency predicted by test (1.03 Hz) lies midway between the rigid slug model frequency (0.738 Hz) and the uniform gravity pendulum model frequency (1.264 Hz). It is also noted that unlike the uniform gravity pendulum and the test data, the mass of the rigid slug model is, of course, constant and equal to the total liquid mass m_L; however, the significant self-inertia of the pendulum mass acts in effect to diminish the net coupling of this model to spin axis rotations.

The first flight data to clearly show the despin loop oscillation frequency together with spin frequency was the power spectrum of the analog control error telemetry recorded on flight F2 and is reproduced in Fig. 7. The rotor slosh mode frequency is plainly evident at 1.03 Hz, the same as predicted by the modal test and analysis. This excellent agreement is perhaps fortuitous, although agreement with the other test data was also quite good, within 3% vs the 65–10% range of fill fractions observed on the F4, as will be shown.

Other Off-Axis Tank Data

There is very little published data on the modes of vibration of the spinning liquid in a partially filled off-axis tank. This is in sharp contrast to the extensive literature on the liquid lateral slosh modes in uniform gravity, largely to support launch vehicle design. The bulk of empirical and theoretical literature on spinning liquids is so absorbed with the determination of interactions at vehicle nutation frequency and, particularly, the energy dissipation that it is of little value for general control system analysis. The principal reference text on the theory of rotating fluids[5] chooses to ignore the partially filled tank apparently because liquid behavior in this case is not strictly limited to rotating media.

The only published theory for the off-axis tank based on the homogeneous vortex assumption was unsuccessful[6] and, in fact, inspired this empirical approach. Another forced motion test program[7] addressed off-axis spherical tanks, but was aimed again at nutation energy dissipation and constrained to sinusoidal excitation. Unpublished finite-element eigenmode modeling for the off-axis case at INTELSAT is beginning to compare well with measured data, promising that spinning liquid modal tests may soon follow rather than lead analysis—as is the practice in the more established area of structural mechanics.

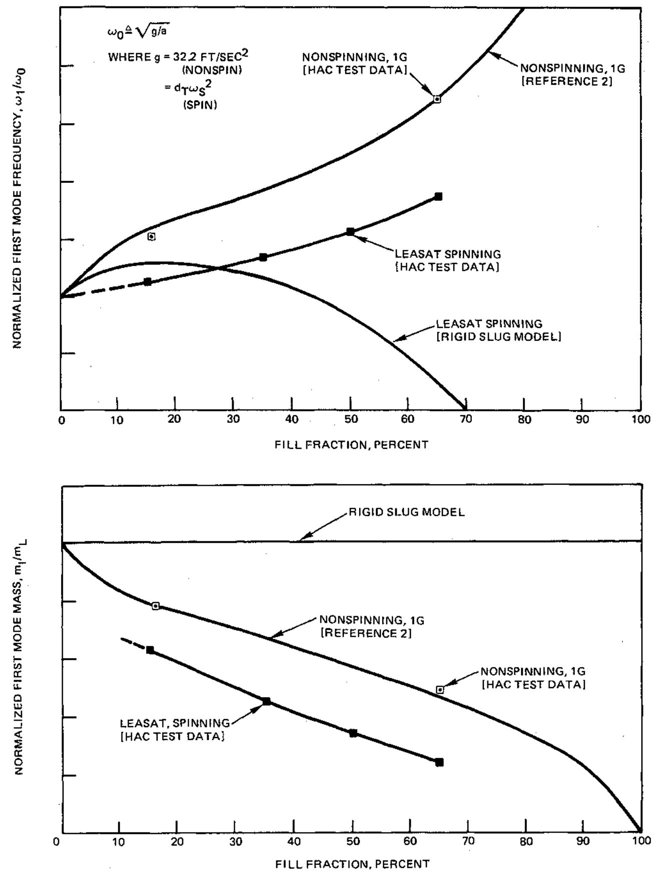

Fig. 6 Trend comparison of LEASAT test data with 1 g and rigid slug models.

Table 1 Comparison of LEASAT rotor azimuth slosh mode frequency predictions at 65% FF

Parameters	Symbol[a]	Rigid slug model	Modal test data	Uniform g model
Pendulum				
Frequency	$\hat{\omega}_1 = \omega_1/\omega_s$	1.556	2.154	2.471
Length	ℓ_1/a	0.265	0.733	0.557
Mass	m_1/M_L	1.00	0.26	0.46
Self-inertia ratio	$\beta = J_1/m_1\ell_1^2$	4.236	0	0
Coupling inertia, slug-ft^2	I_1	851	867	1400
Rotor				
Total propellant mass coupling factor	$\rho = nI_1/I_s$	0.179	0.182	0.294
Rotor mode frequency, Hz	ω_1^*	0.738	1.032	1.264
($\omega_s = 0.43$ Hz)	(r/s)	4.64	6.48	7.94

[a] $\omega_1^* = \omega_1/\sqrt{1-\rho}$ and $I_1 = [(\hat{\omega}_1^2 + 1)/\hat{\omega}_1^2]^2 m_1 d_T^2/(1+\beta)$.

IV. Closed-Loop Interaction Analysis

The analytical model of the despin control system representative of the system's used on the LEASAT and INTELSAT VI class spacecraft is given in Fig. 8. The spacecraft "plant" derived from the linearized equations of motion is represented as two rigid inertias (payload and rotor) with a quadratic pole/zero pair (with zero damping initially assumed) on the rotor representing a propellant slosh mode. Multiple modes are accommodated with a series of cascaded dipole models. Because feedback through the outer loop is weak relative to the inner loop, the analysis to follow will consider only the dominant wider bandwidth inner-loop dynamics. The inner-loop error sampling rate for LEASAT is eight times the relative rate using an eight-pole encoder (much higher than the predicted mode frequencies) and results in a linear system dynamics at the propellant frequencies.

The spacecraft dynamic transfer function relating the bearing axis torque T_{BA} to the relative phase angle θ_R around which the loop is closed is given by

$$\frac{\theta_R}{T_{BA}} = \frac{1+J}{I_p s^2}\left|\frac{s^2+\omega_z^2}{(1-r)s^2+\omega_z^2}\right| \tag{7}$$

where the transfer function zero is given by

$$\omega_z^2 = \left|\frac{1+J}{1+J-\rho}\right|\omega_f^2 \tag{8}$$

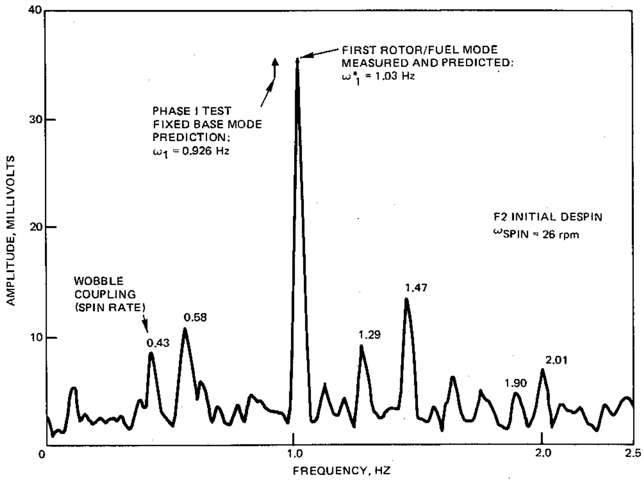

Fig. 7 Amplitude spectrum of LEASAT control loop error telemetry during F2 on-orbit instability.

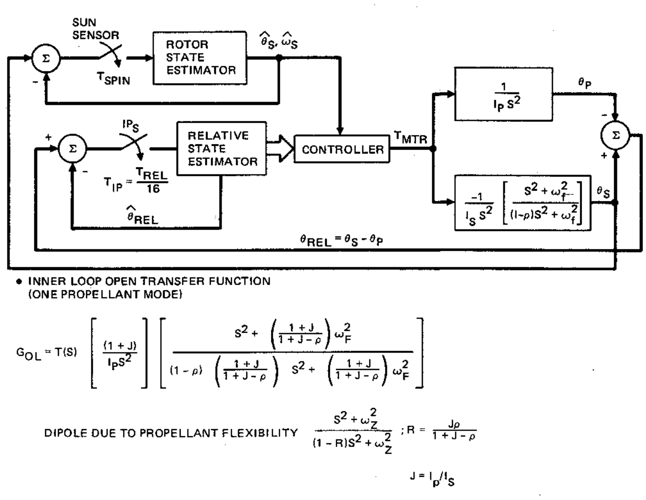

Fig. 8 Analytical model for despin control system.

and the dynamic coupling factor by

$$r = \frac{J\rho}{1+J-\rho} \simeq \left|\frac{I_{\text{fluid}}}{I_{\text{rotor}}}\right| * \left|\frac{I_p}{I_p+I_R}\right| \tag{9}$$

Thus, the propellant slosh pole frequency (the frequency detected by the control system) for $\omega_f = \omega_1$, the first azimuth slosh mode, is given by

$$\omega_p^2 = \frac{\omega_z^2}{(1-r)} = \frac{\omega_1^2}{(1-\rho)} = (\omega_1^*)^2 \tag{10}$$

As was discussed in the previous section, the strength of the propellant mode dynamic coupling to the rotor dynamics is determined by the ratio ρ of the moment of inertia of the liquid mass participating in the mode to the total rotor spin moment of inertia. As can be seen from Eq. (9) this ratio, in conjunction with the relative payload-to-rotor moments of inertia, establishes the spacecraft mode pole-zero separation and thus defines the strength of the coupling to the control system.

The effect of the payload spin moment of inertia on the interaction can also be observed in the expression for the coupling parameter r. For a larger payload MOI (relative to the rotor MOI), the interaction becomes stronger, i.e., as the payload becomes larger relative to the rotor, rotor dynamics become more significant—a "tail wagging the dog" condition. Note also that as $r \to 0$ (weaker coupling) the pole and zero cancel each other, leaving only rigid-body dynamics. Thus, as the propellant load is depleted (or at very high fill fractions), dynamic coupling is reduced. The propellant load at which this coupling is maximized is determined by the rotor liquid mass fraction—a 30% fill fraction for LEASAT.

Using this analytical description of propellant mode dynamics, an analytical model of the control subsystem, and a root perturbation technique developed for predicting the characteristics of control system interactions with both spacecraft nutation and payload flexibility,[3] the behavior of the propellant/control system interaction can be predicted. The closed-form expression for the closed-loop propellant mode damping ratio resulting from control system operation can be shown to be

$$\xi_{cl} = \frac{-r}{2(1-r)^{1/2} * M(A/(1-r),\phi)} \tag{11}$$

where $M(A,\phi)$ consolidates the effect of the control system on the damping ratio and is given by

$$M(A,\phi) = \frac{A\sin\phi}{1+A^2+2A\cos\phi} \tag{12}$$

The parameters A and ϕ represent the control system open-loop gain and phase (exclusive of the propellant dipole), respectively, evaluated at the propellant mode frequency and are determined by control-loop design procedures. The function $M(A,\phi)$ thus describes the relative "tuning" of the control system to the propellant mode.

Note that the basic strength of the interaction (defined by the magnitude of ξ_{cl}) is determined by both the fixed mass property parameter r and the magnitude of $M(A,\phi)$. In addition, since $0 \le r < 1$, the fundamental stability of the interaction (the sign of the damping ratio setting a positive or negative propellant mode exponential) is determined solely by the control system transmission phase characteristic that establishes the sign of $M(A,\phi)$. It can be shown[3] that for a positive ξ_{cl} (hence, a stable interaction in which the control loop provides active propellant damping) the transmission phase angle ϕ at the propellant mode frequency must lie in the third or fourth quadrant, i.e., $0 \ge \phi \ge -180$ deg. A phase angle in the first or second quadrants will always generate an unstable interaction. In addition, it can be shown that the system coupling is weakest for both high and low open-loop gains ($A \gg 1$ or $A \ll 1$).

The effect of passive propellant damping on the interaction can be determined using superposition. The composite damping ratio for a propellant mode with passive damping ξ_p is given by

$$\xi_{\text{net}} = \xi_{\text{cl}} + \xi_p \tag{13}$$

This relationship will be valid for damping ratios much less than unity.[3]

Two design options are available to ensure a stable interaction: phase stabilization and gain stabilization. In phase stabilization, the control system open-loop phase at the mode frequency is adjusted so that $\xi_{\text{cl}} \geq 0$ (i.e., ϕ is forced to lie in the third or fourth quadrant). For phase stabilization, the interaction will be inherently stable (i.e., stable with no assumed passive damping, $\xi_p = 0$) and the control system providing positive active damping. Gain stabilization selects the control-loop gain at the mode frequency to force

$$|\xi_{\text{cl}}| < |\xi_p| \tag{14}$$

when the open-loop phase $\phi \leq -180$ deg. Thus, with gain stabilization, the destabilizing effect of the control system is made to be weaker than the stabilizing effect of passive propellant damping. The inclusion of notch filters in the control shaping can be used to alter the system gain (or phase) in a particular frequency band, without significant disturbance to the other control-loop characteristics.

The resulting predicted closed-loop damping ratio of the first propellant mode for the LEASAT DCS as a function of tank fill fraction is plotted in Fig. 9. Operating at a spin rate of 26 rpm, the phase crossover (-180 deg transition) of the DCS will occur at 5.0 rad/s (or 1.84 times spin rate). Thus, for a propellant mode frequency higher than 5.0 rad/s, the interaction with the DCS is expected to be destabilizing. Using the propellant modal data presented in Sec. III, the lowest expected free mode frequency will be ~2 times spin rate. Thus, for LEASAT a negative damping ratio would be predicted at all tank fill fractions (with the strongest destabilization occurring at a fraction fill of 30%).

Because the open-loop gain at the mode frequency is less than unity (-8 dB), raising the overall loop gain for LEASAT will increase the coupling strength and increase the magnitude of ξ_{cl}. This effect can be seen in the two curves shown in Fig. 9, one representing the response with a single torque motor on and the second plotting the response with both of the redundant torque motors active. For the LEASAT DCS, enabling both motors has the effect of doubling the control gain. The peak negative damping predicted for LEASAT is then 0.37%

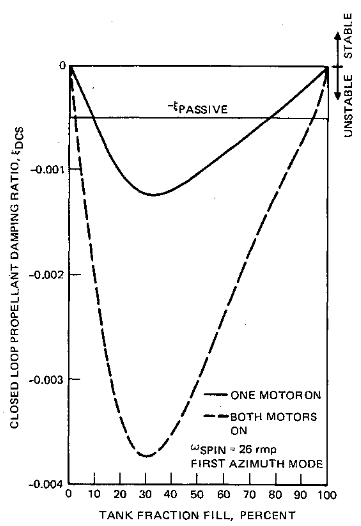

Fig. 9 Predicted closed-loop propellant mode damping ratio as a function of propellant load for LEASAT control system.

with both motors on and 0.12% with one motor on (occurring at a fill fraction of 30%).

In order for a "gain stabilized" condition to exist for LEASAT, the magnitude of ξ_{cl} must be less than the passive fluid damping (measured to be ~0.05%). As shown in Fig. 9, this condition will exist for tank fill fractions below 10% and above 77% with one motor on and below 3% and above 93% if both motors are activated. Between these regions a DCS instability would be expected.

V. On-Orbit Verification Experiments During LEASAT F4 Mission

In conjunction with the previously described analysis and test activities, and because of the potential impact of this phenomenon on other spacecraft, a series of experiments were planned and conducted during transfer orbit operations of the third LEASAT (F4) mission, launched on Sept. 1, 1985. These experiments consisted of measurements of the strength of the control system interaction over a wide range of propellant loads. The fundamental test goal was to validate the parametric data obtained during scale-model testing and the resulting interaction analysis. Specifically, the test objectives were:

1) To measure the free-free propellant slosh mode frequency over a wide range of tank fill fractions.

2) To verify the predicted despin control system stability or instability over a range of fill fractions.

3) To measure the closed-loop propellant mode damping ratio (ξ_{cl}, quantifying the strength of interaction and the predicted value of participating liquid mass. Measurements were to be made with both one and two motor drivers on (a control-loop gain variation of 2 : 1).

4) To measure propellant passive damping in the unbaffled, 36 in. diameter tanks.

The experiments were conducted prior to apogee motor firing (AMF) at a tank fraction fill of 62% and following each of the four AMF burns (at fill fractions of 36, 25, 10.5, and 2.5%). Individual tests consisted of inertially despinning the platform in the sun reference mode with either one or both motor drivers on and observing the response of the tracking loop error, commanded motor voltage, and motor current telemetry channels, along with the rotor spin rate as measured by the spin period (sun pulse to sun pulse time interval) telemetry. The tracking loop error telemetry on LEASAT is sampled four times each minor telemetry frame, giving a sampling rate of 3.91 Hz or a frequency measurement bandwidth of 1.95 Hz.

Propellant mode instability was observed as an exponential growth on all four telemetry channels. Growth was limited due to saturation of the motor driver. The divergence time constant in the linear range and oscillation frequency (measured on the control-loop error telemetry) were used to compute the closed damping ratio. Passive fuel damping ξ_p was measured by opening the control loop (switching to ground torque mode) and measuring the decay rate of the propellant-induced rotor oscillations (using spin period measurement data). The control system interaction alone was determined using superposition.

The results of the F4 tests are summarized in Table 2, with the strip chart time history data from one such test given in Fig. 10. All but one experiment was carried out successfully. At the 25% fill fraction condition, the large rotor unbalance (resulting from burning 75% of the propellant with the propellant tank crossover valves closed) caused a large spin axis wobble (~1 deg) and a resulting saturation of the motor driver (due to coupling through the platform imbalance). Thus, the dominant spin frequency control error signal did not permit linear operation and no instability was observed.

As can be seen in Table 2, the predicted instability was verified at all other experiment fraction fills. The observed free-free mode frequencies of the lateral slosh modes were within 3% of the predicted value. Passive propellant damping of ~0.05% was observed at all fraction fills. Damping ratio measurement accuracy was limited by telemetry quantization and signal-to-noise limitations. Differences between predicted

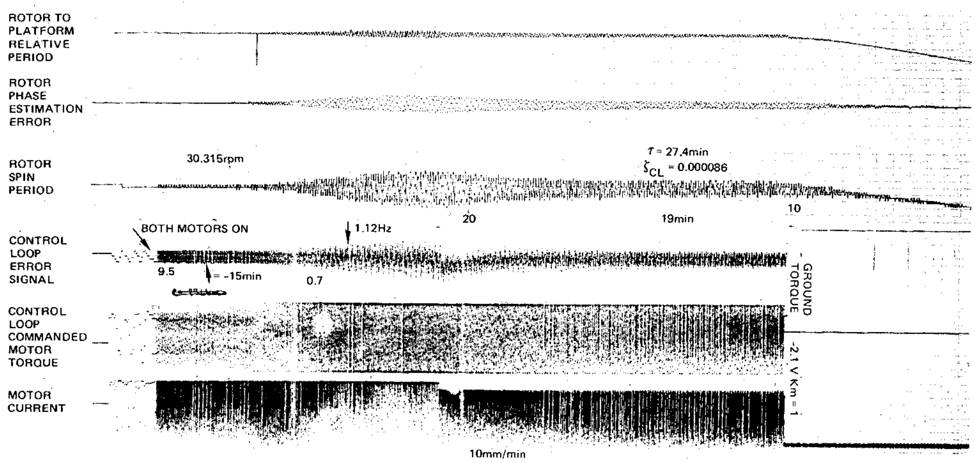

Fig. 10 Spacecraft telemetry during LEASAT on-orbit propellant interaction experiment (36% propellant load).

Table 2 LEASAT F4 on-Orbit Propellant Interaction Experiment Data

Condition	Fraction fill, %	Spin rate, rpm	Measured propellant mode frequency (free-free), Hz	Measured f_m/f_{spin} (free-free)	IR&D predict f_m/f_{spin} (free-free)	Fuel damping ξ_f, %	Control loop interaction: $\xi_{cl} = \xi_{measured} - \xi_f$		
								One motor on, %	Both motors on, %
Pre-AMF 1	62	28.531	1.11	2.33	2.30	0.05	On-orbit	−0.06	−0.12
							Predict	−0.08	−0.22
Pre-AMF 2	36	30.315	1.12	2.22	2.21	0.05	On-orbit	−0.04	−0.07
							Predict	−0.12	−0.32
Pre-AMF 3	25	—	(no data obtained due to wobble cross coupling)						
Pre-AMF 4	10.5	28.159	0.96	2.05	1.99	0.05	On-orbit	−0.01	−0.14
							Predict	−0.05	−0.19
Post-AMF 4	2.5	—	—	—	—	—		(stable coupling)	

and measured damping ratios can also be attributed to control electronics circuit parameter deviations from nominal which can alter the values of A and ϕ (no additional work has been done to "fine tune" the predictions).

Significant conclusions which can be drawn from the experiments are:

1) The basic analytical modeling of lateral slosh mode dynamics was verified.

2) The scale-model test data provided highly accurate mode frequency and mass predictions.

3) The analytical technique to predict control system interaction was validated. The demonstrated significant increase in coupling strength at higher control gains (for LEASAT) is supported by analysis.

4) The interaction at 10.5% fill fraction demonstrated the effect of a "gain-stabilized" mode where the basic interaction is destabilizing but the strength of the interaction is weaker than the passive propellant damping, yielding a net stable interaction. In addition, the increase in coupling strength with higher loop gain was demonstrated by the transition to instability with both motors on.

VI. Conclusions

This paper has presented the results of a study to investigate potential interactions between the payload control system and propellant slosh modes in dual-spin spacecraft. The interaction phenomenon was identified as the source of the instability observed during transfer orbit operations of the LEASAT spacecraft. Ground scale-model testing was shown to accurately define critical mode parameters. Dynamic modeling and analytical design techniques have been presented that permit accurate predictions of fluid behavior in the presence of active control and that can be used to develop control system designs to ensure stability. On-orbit testing verified the basic analytical and test results.

While this paper has placed emphasis on the interaction between the lateral slosh modes and the payload despin control system, elevation modes within the propellant have also been studied and are of concern. Vehicle spin axis coning in response to elevation slosh modes have been shown to interact with the nutation stabilization system for a vehicle spinning about a minimum moment of inertia. This system typically utilizes a rotor-mounted linear accelerometer to sense nutation and generate thruster firing commands to remove transient nutation and maintain attitude stability. Additional work has also been carried out to evaluate the effect of elevation modes on spin axis pointing accuracy during thruster maneuver transients.

References

[1]Slafer, L. I., "Attitude and Payload Control System for the LEASAT Naval Communications Satellite," Paper presented at AAS Rocky Mountain Guidance and Control Conference, Feb. 1982.

[2]Abramson, H. N. (ed.), *The Dynamic Behavior of Liquids in Moving Containers—With Applications to Space Vehicle Technology*, NASA SP-106, 1966.

[3]Slafer, L. I. and Marbach, H. D., "Active Control of the Dynamics of a Dual-Spin Spacecraft," *Journal of Spacecraft and Rockets*, Vol. 12, May 1975, pp. 287–293.

[4]Brown, D. L., et al., "Parameter Estimation Techniques for Modal Analysis," Society of Automotive Engineers Paper 790221, Feb. 1979.

[5]Greenspan, H. P., *The Theory of Rotating Fluids*, Cambridge University Press, Cambridge, England, 1969.

[6]El-Raheb, M. and Wagner, P., "Vibration of a Liquid with a Free Surface in a Spinning Spherical Tank," *Journal of Sound and Vibration*, Vol. 76, No. 1, pp. 83–93, 1981.

[7]Zedd, M. F. and Dodge, F. T., "Energy Dissipation of Liquids in Nutating Spherical Tanks Measured by a Forced Motion Spin Table," AIAA Paper 84-1842, Aug. 1984.